



Measuring In-Flight Angular Motion With a Low-Cost Magnetometer

by Thomas E. Harkins and Michael J. Wilson

ARL-TR-4244

September 2007

NOTICES

Disclaimers

The findings in this report are not to be construed as an official Department of the Army position unless so designated by other authorized documents.

Citation of manufacturer's or trade names does not constitute an official endorsement or approval of the use thereof.

DESTRUCTION NOTICE—Destroy this report when it is no longer needed. Do not return it to the originator.

Army Research Laboratory

Aberdeen Proving Ground, MD 21005-5069

ARL-TR-4244

September 2007

Measuring In-Flight Angular Motion With a Low-Cost Magnetometer

Thomas E. Harkins
Weapons and Materials Research Directorate, ARL

Michael J. Wilson
ATK

REPORT DOCUMENTATION PAGE

Form Approved
OMB No. 0704-0188

Public reporting burden for this collection of information is estimated to average 1 hour per response, including the time for reviewing instructions, searching existing data sources, gathering and maintaining the data needed, and completing and reviewing the collection information. Send comments regarding this burden estimate or any other aspect of this collection of information, including suggestions for reducing the burden, to Department of Defense, Washington Headquarters Services, Directorate for Information Operations and Reports (0704-0188), 1215 Jefferson Davis Highway, Suite 1204, Arlington, VA 22202-4302. Respondents should be aware that notwithstanding any other provision of law, no person shall be subject to any penalty for failing to comply with a collection of information if it does not display a currently valid OMB control number.

PLEASE DO NOT RETURN YOUR FORM TO THE ABOVE ADDRESS.

1. REPORT DATE (DD-MM-YYYY) September 2007		2. REPORT TYPE Final		3. DATES COVERED (From - To) 2006-2007	
4. TITLE AND SUBTITLE Measuring In-Flight Angular Motion With a Low-Cost Magnetometer				5a. CONTRACT NUMBER	
				5b. GRANT NUMBER	
				5c. PROGRAM ELEMENT NUMBER	
6. AUTHOR(S) Thomas E. Harkins (ARL) and Michael J. Wilson (ATK)				5d. PROJECT NUMBER 1L162618AH80	
				5e. TASK NUMBER	
				5f. WORK UNIT NUMBER	
7. PERFORMING ORGANIZATION NAME(S) AND ADDRESS(ES) U.S. Army Research Laboratory Weapons and Materials Research Directorate Aberdeen Proving Ground, MD 21005-5066				8. PERFORMING ORGANIZATION REPORT NUMBER ARL-TR-4244	
9. SPONSORING/MONITORING AGENCY NAME(S) AND ADDRESS(ES)				10. SPONSOR/MONITOR'S ACRONYM(S)	
				11. SPONSOR/MONITOR'S REPORT NUMBER(S)	
12. DISTRIBUTION/AVAILABILITY STATEMENT Approved for public release; distribution is unlimited.					
13. SUPPLEMENTARY NOTES					
14. ABSTRACT A technique for obtaining pitch, yaw, and roll rates of a projectile from a single, low-cost, commercial off-the-shelf magnetometer has been developed at the Advanced Munitions Concepts Branch of the U.S. Army Research Laboratory's Weapons and Materials Research Directorate. In this report, the magnetometer-based methodology is presented, the flight experiment and subsequent analyses are described, criteria for use of this methodology are given, and the potential uses of this technique in inertial measurements unit/INS applications are discussed.					
15. SUBJECT TERMS high g; magnetometer; pitch; projectile dynamics; projectile navigation; strap-down sensors; telemetry; yaw					
16. SECURITY CLASSIFICATION OF:			17. LIMITATION OF ABSTRACT	18. NUMBER OF PAGES	19a. NAME OF RESPONSIBLE PERSON
a. REPORT Unclassified	b. ABSTRACT Unclassified	c. THIS PAGE Unclassified	SAR	20	Thomas E. Harkins
			19b. TELEPHONE NUMBER (Include area code) 410-306-0850		

Contents

List of Figures	iv
1. Introduction	1
2. Inertial Navigation of Projectiles	1
3. Vector Magnetometer	4
4. Obtaining Angular Rates From Vector Magnetometers	4
5. Obtaining Spin Rate From Magnetometers	5
6. Measuring Angular Rates of a NASA Crew Exploration Vehicle (CEV) Model	6
7. Criteria for the Use of Magnetometer-Based Angular Rate Estimation	9
8. Summary	10
9. References	11
Distribution List	12

List of Figures

Figure 1. Coordinate systems.....	2
Figure 2. Earth-fixed and body-fixed systems and the Euler angle rotation.	3
Figure 3. NASA re-entry vehicle models with sensor and telemetry system.	7
Figure 4. Apollo model flight data.....	7
Figure 5. Pitch rate history from rate sensors and magnetometers.	8
Figure 6. Elevation (θ) and azimuth (ψ) angle history.	9

1. Introduction

The Advanced Munitions Concepts Branch of the U.S. Army Research Laboratory's (ARL's) Weapons and Materials Research Directorate has for many years designed, built, and employed body-fixed sensor and telemetry systems to measure flight body kinematics, primarily in support of military ordnance testing. Because requirements imposed by military applications such as high-g environment, extreme projectile dynamics, small size, low cost, low power consumption, etc., exclude many traditional inertial sensor systems, ARL is continually exploring emerging technologies and developing alternate techniques for their utility in obtaining desired measurements.

With the result from vector differentiation relating the time derivatives of a vector represented in two coordinate systems in relative motion, a technique for obtaining pitch, yaw, and roll rates from a single, low-cost, commercial off-the-shelf magnetometer was developed. In a recent ARL flight experiment intended to characterize the angular motion of National Aeronautics and Space Administration (NASA) re-entry capsules, no data were available from the strap-down angular rate sensors during critical portions of several flights because the launch environment and projectile dynamics exceeded sensor capabilities. These rates were successfully derived from magnetometer data, and complete Euler angular histories of the test trajectories were obtained with an ARL-developed vector-matching algorithm.

In this report, the magnetometer-based methodology is presented, the flight experiment and subsequent analyses are described, criteria for use of this methodology are given, and potential uses of this technique in inertial measurement unit (IMU)/inertial navigation system (INS) applications are discussed.

2. Inertial Navigation of Projectiles

The equations of motion describing free-flight dynamics of rigid projectiles have six degrees of freedom, three translational velocity components and three rotational velocity components. A traditional strap-down IMU consists of an orthogonal triad of linear accelerometers and an orthogonal triad of angular rate sensors oriented along a projectile's principal axes. Given initial launch position, orientation, and velocity of a projectile, the rate sensors' output is integrated to update the projectile orientation, and the accelerometers are integrated once to update the projectile velocity and twice to update the projectile position. The solution of the inertial navigation problem is conceptually simple, but it is often difficult to realize an IMU capable of measuring the required six body states under constraints imposed by a particular application. Although this problem is

equally of concern to accelerometers and rate sensors, only the orientation estimation (i.e., rate sensor) problem is addressed herein.

Formulation of the inertial navigation problem for gun- and tube-launched projectiles requires the use of multiple coordinate systems (Harkins, 2003, 2007). Trajectory time histories are best described in an earth-fixed coordinate system with its origin at the launcher. Of necessity, strap-down sensor measurements are made in a flight-body-fixed coordinate system, and target locations are most naturally described in another earth-fixed system.

The first coordinate system is right-handed Cartesian (I, J, K) with its origin at the launch site. This will be referred to as the “earth-fixed” system and the axes are defined by

- The I and J axes, which define a plane tangent to the earth’s surface at the origin;
- The K axis, which is perpendicular to the earth’s surface with positive downward, i.e., in the direction of gravity;
- The I axis, which is chosen so that the centerline of the launcher is in the $I-K$ plane.

Down-range travel is then measured along the I axis, deflection along the J axis (positive to the right when one is looking down range), and altitude along the K axis (positive downwards) (see figure 1).

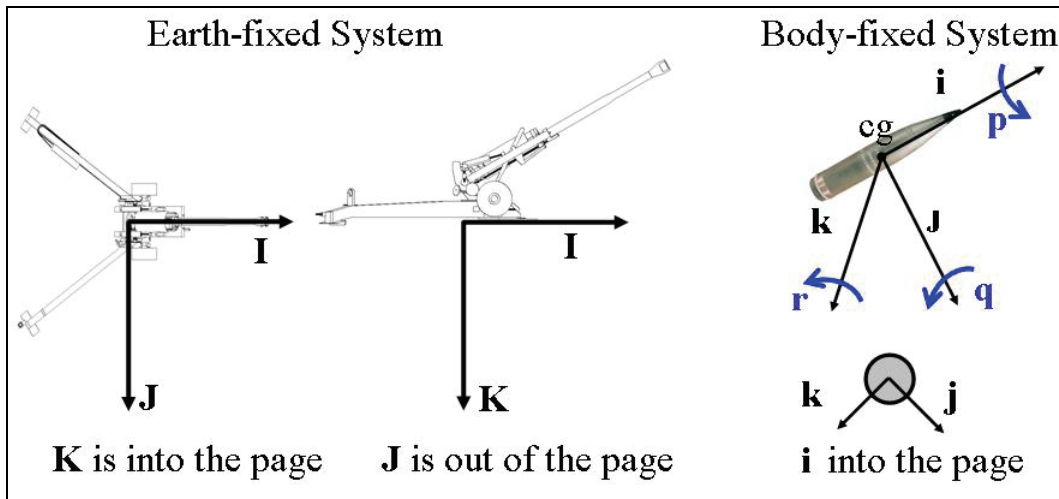


Figure 1. Coordinate systems.

The second system is convenient for aeroballistic computations of rigid projectiles’ flights and for describing the locations and orientations of such projectiles’ components. This system is right-handed Cartesian (i, j, k) with its origin at the center of gravity (c.g.) of the flight body. For rotating flight bodies, the projectile-fixed coordinate system usually has its i axis lying along the projectile axis of symmetry, i.e., the spin axis (with positive in the direction of travel at launch). The j and k axes are then oriented so as to complete the right-handed orthogonal system (figure 1). Spin (p),

pitch (q), and yaw (r) rates are measured about these axes. This will be referred to as the “body-fixed” system.

The third coordinate system (X, Y, Z) is commonly employed to specify locations on or near the earth’s surface, i.e., north, east, and down. This will be referred to as the “navigation” system where north = X , east = Y , and down = Z .

The earth-fixed and body-fixed coordinate systems are related through an Euler rotation sequence, beginning with a rotation of the earth-fixed frame about the K -axis through the yaw angle ψ . The system is then rotated about the new J' -axis through the pitch angle θ . Finally, the system is rotated about the new i -axis through the roll angle ϕ . The two systems are related by the direction cosine transformation matrix (DCM), T_{Eb} , with the subscript denoting earth fixed to body fixed.

This transformation matrix is

$$T_{Eb} = \begin{pmatrix} c_\psi c_\theta & s_\psi c_\theta & -s_\theta \\ c_\psi s_\theta s_\phi - s_\psi c_\phi & s_\psi s_\theta s_\phi + c_\psi c_\phi & c_\theta s_\phi \\ c_\psi s_\theta c_\phi + s_\psi s_\phi & s_\psi s_\theta c_\phi - c_\psi s_\phi & c_\theta c_\phi \end{pmatrix}, \quad (1)$$

where c_\bullet is $\cos(\bullet)$, and s_\bullet is $\sin(\bullet)$. Figure 2 shows both coordinate systems and the Euler angle relations between them.

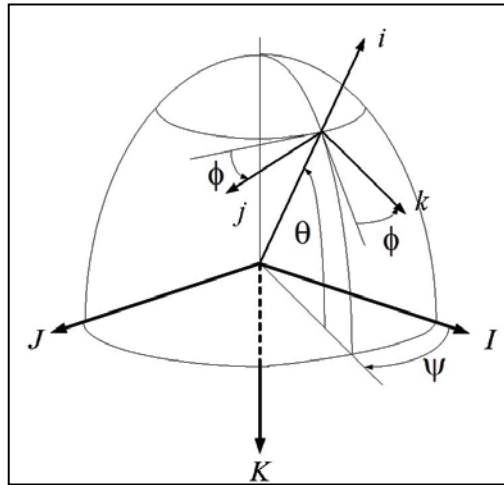


Figure 2. Earth-fixed and body-fixed systems and the Euler angle rotation.

The body-fixed components of projectile angular motion and the Euler angle derivatives are related by

$$\begin{aligned} \dot{\phi} &= p + [q \sin(\phi) + r \cos(\phi)] \tan(\theta) \\ \dot{\theta} &= q \cos(\phi) - r \sin(\phi) \\ \dot{\psi} &= (q \sin(\phi) + r \cos(\phi)) / \cos(\theta) \end{aligned} \quad (2)$$

3. Vector Magnetometer

Among the many varieties of magnetic sensors, “vector” magnetometers are devices whose output is proportional to the magnetic field strength along the sensor’s axis(es). If a tri-axial vector magnetometer is installed so that the sensor axes are parallel to the axes of the body-fixed system, the projections of the earth’s magnetic field onto each of the sensor axes can be obtained by equation 1. If $\vec{M}_E = (M_I, M_J, M_K)$ is the magnetic field vector in the earth-fixed system, then the components along the sensor axes are given by

$$\vec{M}_b = T_{Eb} \vec{M}_E \quad (3)$$

$$\begin{aligned} M_i &= c_\psi c_\theta M_I + s_\psi c_\theta M_J - s_\theta M_K \\ \text{or} \quad M_j &= (c_\psi s_\theta s_\phi - s_\psi c_\phi) M_I + (s_\psi s_\theta s_\phi + c_\psi c_\phi) M_J + c_\theta s_\phi M_K \\ M_k &= (c_\psi s_\theta c_\phi + s_\psi s_\phi) M_I + (s_\psi s_\theta c_\phi - c_\psi s_\phi) M_J + c_\theta c_\phi M_K \end{aligned} \quad (4)$$

In any real magnetic sensor, determination of axes’ orientations and calibration coefficients can be a complex process, but for the present purpose, it is assumed that this has been successfully accomplished and \vec{M}_b is being accurately measured at a known sampling rate.

4. Obtaining Angular Rates From Vector Magnetometers

Consider two coordinate systems with the same origin and in relative motion, e.g., the earth-fixed and body-fixed systems just described at the time of projectile launch. From vector differentiation, the time derivative of any vector in the earth-fixed system ($\dot{\vec{v}}_E = \delta \vec{v}_E / \delta t$) and its time derivative in the body-fixed system ($\dot{\vec{v}}_b = \delta \vec{v}_b / \delta t$) are related by

$$\dot{\vec{v}}_E = \dot{\vec{v}}_b + \vec{\omega}_b \times \vec{v}_b \quad (5)$$

where $\vec{\omega}_b = (p, q, r)$. Applied to the geomagnetic field vector, equation 5 becomes

$$\dot{\vec{M}}_E = \dot{\vec{M}}_b + \vec{\omega}_b \times \vec{M}_b \quad (6)$$

Realizing that equation 6 is unaffected by a translation of the earth-fixed system’s origin to the projectile c.g. at each sampling time and that \vec{M}_E is unchanging in the earth-fixed system and expanding in component form, we have the relations

$$\dot{M}_i = -qM_k + rM_j, \quad \dot{M}_j = pM_k - rM_i, \quad \text{and} \quad \dot{M}_k = -pM_j + qM_i. \quad (7)$$

Because these equations are not linearly independent, they can not be solved directly for the angular rates. However, for most rolling projectiles where $|p| \gg |q|$ and $|r|$, a good estimate of p is readily obtainable from the magnetometer data, as described in the next section. With a spin estimate, this system can be solved to yield estimates of the body-fixed pitch and yaw rates. Therefore,

$$\hat{q} = (\dot{M}_k + pM_j)/M_i \quad \text{and} \quad \hat{r} = (-\dot{M}_j + pM_k)/M_i. \quad (8)$$

5. Obtaining Spin Rate From Magnetometers

Consider an earth-fixed, right-handed Cartesian coordinate system where the z-axis is along the geomagnetic field. In this new system, denoted by the subscript m , the geomagnetic field vector is $\vec{M}_m = (0, 0, |\vec{M}_E|)^T$. As seen in section 2, there is a new set of Euler angles that defines a transformation matrix from this magnetic coordinate system into the body-fixed system so that

$$\begin{pmatrix} M_i \\ |\vec{M}_E| \\ M_j \\ |\vec{M}_E| \\ M_k \\ |\vec{M}_E| \end{pmatrix} = \begin{pmatrix} c_{\psi_m} c_{\theta_m} & s_{\psi_m} c_{\theta_m} & -s_{\theta_m} \\ c_{\psi_m} s_{\theta_m} s_{\phi_m} - s_{\psi_m} c_{\phi_m} & s_{\psi_m} s_{\theta_m} s_{\phi_m} + c_{\psi_m} c_{\phi_m} & c_{\theta_m} s_{\phi_m} \\ c_{\psi_m} s_{\theta_m} c_{\phi_m} + s_{\psi_m} s_{\phi_m} & s_{\psi_m} s_{\theta_m} c_{\phi_m} - c_{\psi_m} s_{\phi_m} & c_{\theta_m} c_{\phi_m} \end{pmatrix} \begin{pmatrix} 0 \\ 0 \\ 1 \end{pmatrix} = \begin{pmatrix} -s_{\theta_m} \\ c_{\theta_m} s_{\phi_m} \\ c_{\theta_m} c_{\phi_m} \end{pmatrix} \quad (9)$$

This gives a definition of the magnetometer measurements in terms of the magnetic Euler angles. The magnetic pitch angle,

$$\theta_m = \sin^{-1}(-M_i/|\vec{M}_E|), \quad (10)$$

is the complement of the angle between the projectile's spin axis (\vec{i}), and the magnetic field, \vec{M}_E . The magnetic roll angle, ϕ_m , is computed by

$$\phi_m = \tan^{-1}(M_j/M_k) \quad (11)$$

Analogous to equation 2, the body-fixed rates and the derivatives of the magnetic Euler angles are related by

$$\begin{aligned} \dot{\phi}_m &= p + [q \sin(\phi_m) + r \cos(\phi_m)] \tan(\theta_m) \\ \dot{\theta}_m &= q \cos(\phi_m) - r \sin(\phi_m) \\ \dot{\psi}_m &= (q \sin(\phi_m) + r \cos(\phi_m)) / \cos(\theta_m) \end{aligned} \quad (12)$$

Estimates of $\dot{\phi}_m$ can be obtained in several ways. The simplest method is to make roll period estimates from successive zero crossings or signal extrema on the M_j or M_k signals. This process yields average roll rates over the respective periods. More continuous, higher order estimates are obtained by the computation of equation 11 at each sampling time and the differentiation of the results. Alternatively, $\dot{\phi}_m$ is computed directly from

$$\frac{\delta \tan^{-1}(M_j/M_k)}{\delta T} = \frac{\delta(M_j/M_k)}{\delta T} \left(\frac{1}{1+(M_j/M_k)^2} \right) = \left(\frac{\dot{M}_j M_k - \dot{M}_k M_j}{M_j^2 + M_k^2} \right) \quad (13)$$

with the advantage of avoiding potential singularities in equation 11 when $M_k = 0$. The spin rate (p) can then be estimated by low-pass filtering of the $\dot{\phi}_m$ estimates (Wilson, 2004).

6. Measuring Angular Rates of a NASA Crew Exploration Vehicle (CEV) Model

NASA needs to characterize the aerodynamics of the CEV that will be a part of future Mars missions. Some previous measurements had been made in spark ranges with scale models of the CEV, but this methodology cannot be employed to characterize all conditions of interest because of velocity and stability limitations imposed by safety considerations in an indoor range. Further, only limited amounts of data are collected for each shot in a spark range, so testing costs quickly mount with the number of shots required. With the dual hope of expanding the set of potentially measurable flight dynamics and reducing testing costs, it was decided that gun launching of Mars CEV models equipped with a sensor and telemetry system (figure 3c) at an outdoor range would be explored as a practicable way to acquire the desired data at reentry velocities (Brown et al., 2006). Before proceeding to the Orion CEV tests, we evaluated the proposed methodology using an Apollo capsule model with known aerodynamics (figure 3a and b). The sensor system consisted of six angular rate sensors and a three-axis magnetometer. Along each of the principal axes there were an angular rate sensor with a dynamic range of ± 1000 deg/s, an angular rate sensor with a dynamic range of ± 2000 deg/s, and a vector magnetometer.

Figure 4 gives the body-fixed pitch axis rate sensor data for the first 0.5 second of one of the Apollo model flight tests. Two “problems” with these data are readily apparent. First, the pitch (and yaw) angular rates exceeded the dynamic range of the rate sensors and clipping resulted. Second, after gun launch, the rate sensors required time to “settle”. This is obvious in the 1000-deg/s sensor data but was later discovered to be equally true of the 2000-deg/s sensor data. Because of these issues, the magnetometer-based method was used to estimate the angular rates and the Apollo model’s attitude history.

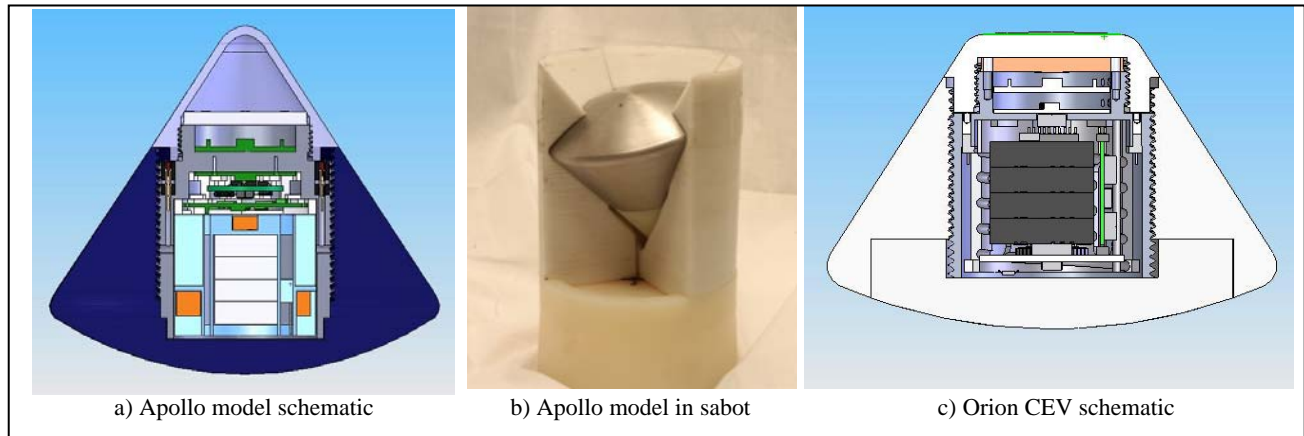


Figure 3. NASA re-entry vehicle models with sensor and telemetry system.

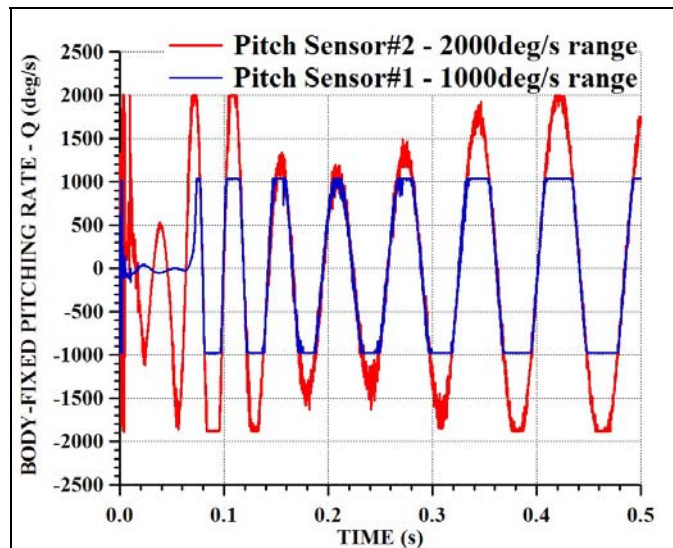


Figure 4. Apollo model flight data.

Initial spin rate was estimated to be approximately 2 Hz from a period measurement of radial magnetometer output. With this value for p , equation 8 was evaluated to obtain estimates of the body-fixed pitch (\hat{q}) and yaw (\hat{r}) rates. We estimated \dot{M}_j and \dot{M}_k by differencing the successive magnetometer measurements. The resulting pitch rate estimate is seen in figure 5a superimposed on the rate sensor data. The good agreement of the magnetometer-derived pitch rate with the rate-sensor-measured pitch rates whenever those measurements exist supports the accuracy of the magnetometer-derived rate estimates at all other times. The magnetometer-derived rates indicate initial pitching rates of approximately 4000 deg/s. These early data are particularly important because the high-drag shape of the model causes the mach 3.5 launch velocity to decay to subsonic speed in less than 1 second, and the high mach numbers are representative of re-entry velocities. Later in the flight, as the model begins to tumble, pitch rates approaching 20000 deg/s are estimated by the magnetometer (figure 5b). Although these data are not of interest for characterizing

CEV aerodynamics, they demonstrate that the magnetometer method does not suffer from dynamic range limitations.

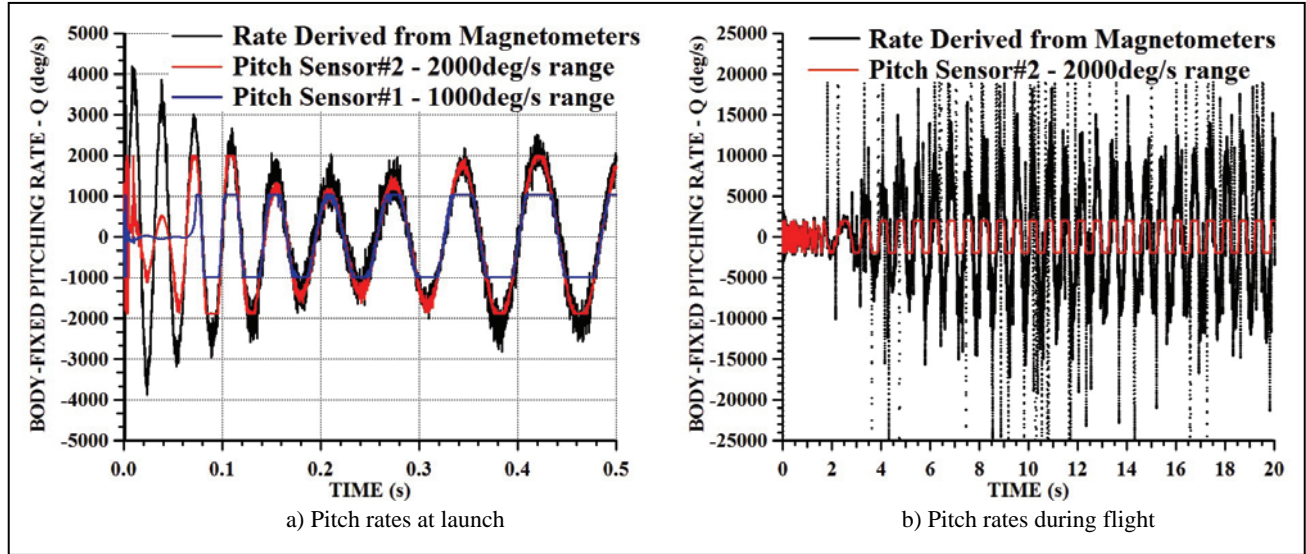


Figure 5. Pitch rate history from rate sensors and magnetometers.

With θ_m , ϕ_m , \hat{q} , and \hat{r} in hand, equation 12 is used to compute $\dot{\psi}_m$ at each sampling interval. The magnetic azimuth is then given by

$$\psi_m(t) = \psi_m(0) + \int_0^t \dot{\psi}_m(t) \delta t . \quad (14)$$

Finally, the earth-fixed Euler angles are given by

$$\begin{pmatrix} \theta \\ \psi \\ \phi \end{pmatrix} = T_{mE} \begin{pmatrix} \theta_m \\ \psi_m \\ \phi_m \end{pmatrix} \quad (15)$$

where T_{mE} is the DCM relating the magnetic and earth-fixed coordinate systems. This methodology has been successfully implemented in an on-board digital signal processor for real-time guidance of experimental projectiles, as reported in reference 1. When this methodology was executed during post-processing of the flight telemetry data, the Apollo model heading history seen in figure 6 was computed for the first second of flight. With these data, aerodynamic coefficients of interest were estimated for the test vehicle, and the flight experiment evaluation was successfully completed.

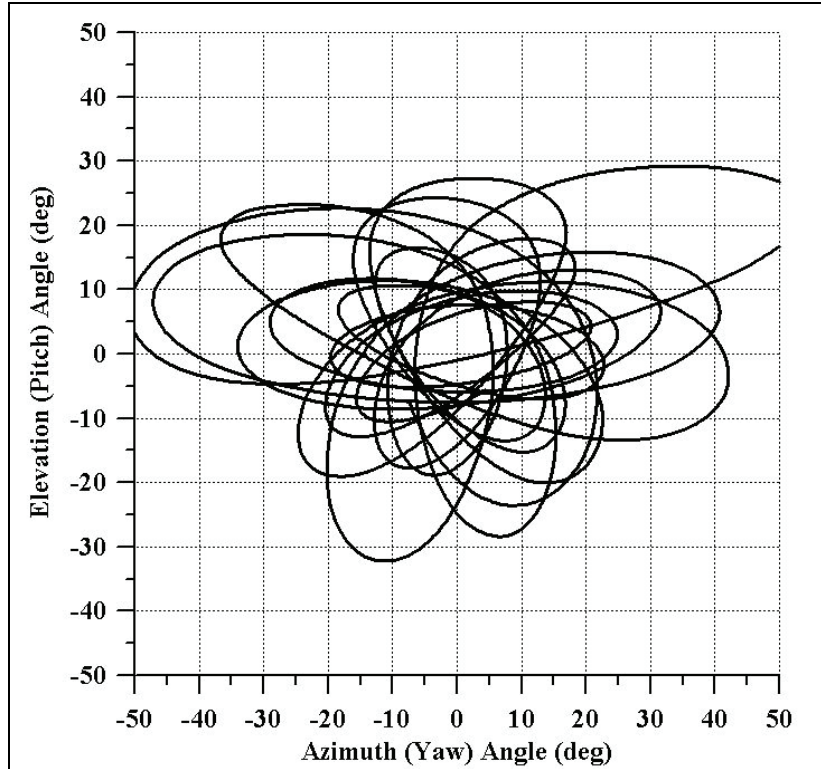


Figure 6. Elevation (θ) and azimuth (ψ) angle history.

7. Criteria for the Use of Magnetometer-Based Angular Rate Estimation

The effectiveness of this methodology is clearly dependent on the accuracy of the measurements of M_i , M_j , M_k , \dot{M}_j , and \dot{M}_k . Thus, a calibrated vector magnetometer is required. Calibration constants can be determined on the ground and pre-loaded or often can be dynamically determined in flight. We estimated \dot{M}_j and \dot{M}_k by differencing successive magnetometer measurements.

This simplistic method requires that data rates be sufficiently high to accurately estimate the derivatives. Sampling rates of at least one sample per degree of projectile rotation have been found to be adequate for a number of simulated projectiles. Alternatively, polynomial fitting to the magnetometer data followed by analytic differentiation has been shown to produce equally accurate results at lower sampling rates. Preferred methods should be determined for individual applications.

8. Summary

Free flight angular dynamics of projectiles have been successfully measured with vector magnetometers in flight experiments during intervals when angular rate sensors have failed to provide measurements. This result argues for investigation of the inclusion of magnetometers as supplements and/or replacements to rate sensors in low-cost IMU/INS systems.

9. References

- Brown, T. G.; Brandon, F.; Bukowski, E.; Davis, B.; Hall, R.; Hathaway, W.; Muller, P.; Topper, B.; Rodgers, A.; Vong, T. Calculating Aerodynamic Coefficients for a NASA Body Using Telemetry Data From Free Flight Range Testing. *57th Aeroballistic Range Association Meeting*, Venice, Italy, September 2006.
- Harkins, T. *Understanding Body-Fixed Sensor Output From Projectile Flight Experiments*; ARL-TR-3029; U.S. Army Research Laboratory: Aberdeen Proving Ground, MD, September 2004.
- Harkins, T. *Solving for Flight Body Angular Histories With the Use of Solar and Magnetic Sensor Data*; ARL-TR-4072; U.S. Army Research Laboratory: Aberdeen Proving Ground, MD, April 2007.
- Wilson, M. *Attitude Determination With Magnetometers for Gun-Launched Munitions*; ARL-TR-3209; U.S. Army Research Laboratory: Aberdeen Proving Ground, MD, August 2004.

NO. OF
COPIES ORGANIZATION

1 DEFENSE TECHNICAL
(PDF INFORMATION CTR
Only) DTIC OCA
8725 JOHN J KINGMAN RD
STE 0944
FORT BELVOIR VA 22060-6218

1 US ARMY RSRCH DEV & ENGRG CMD
SYSTEMS OF SYSTEMS
INTEGRATION
AMSRD SS T
6000 6TH ST STE 100
FORT BELVOIR VA 22060-5608

1 DIRECTOR
US ARMY RESEARCH LAB
IMNE ALC IMS
2800 POWDER MILL RD
ADELPHI MD 20783-1197

1 DIRECTOR
US ARMY RESEARCH LAB
AMSRD ARL CI OK TL
2800 POWDER MILL RD
ADELPHI MD 20783-1197

2 DIRECTOR
US ARMY RESEARCH LAB
AMSRD ARL CI OK T
2800 POWDER MILL RD
ADELPHI MD 20783-1197

3 DIR US ARMY RSCH LABORATORY
ATTN AMSRD ARL SE RL M DUBEY
B PIEKARSKI
AMSRD ARL SE EE Z SZTANKAY
2800 POWDER MILL RD
ADELPHI MD 20783-1197

2 DIR US ARMY RSCH LABORATORY
ATTN AMSRD ARL SE S J EICKE
AMSRD ARL SE SA J PRICE
2800 POWDER MILL RD
ADELPHI MD 20783-1197

3 DIR US ARMY RSCH LABORATORY
ATTN AMSRD ARL SE SS LADAS
A EDELSTEIN D FLIPPEN
2800 POWDER MILL RD
ADELPHI MD 20783-1197

1 DIR US ARMY RSCH LABORATORY
ATTN AMSRD ARL WM MB A FRYDMAN
2800 POWDER MILL RD
ADELPHI MD 20783-1197

NO. OF
COPIES ORGANIZATION

5 CDR US ARMY TACOM ARDEC
ATTN AMSRD AAR AEP F(A) W KONICK
C ROBINSON M D'ONOFRIO
D WARD B CHRISTOPHERSON
2800 POWDER MILL RD
ADELPHI MD 20783-1197

1 DIR US ARMY CECOM RDEC
ATTN AMSEL RD C2 CS J VIG
FORT MONMOUTH NJ 07703-5601

1 CDR US ARMY TACOM ARDEC
ATTN AMSRD AAR QEM E M BOMUS
BLDG 65S
PICATINNY ARSENAL NJ 07806-5000

4 CDR US ARMY TACOM ARDEC
ATTN AMSRD AAR AEM A S CHUNG
W KOENIG W TOLEDO
T RECCHIA
BLDG 95
PICATINNY ARSENAL NJ 07806-5000

1 CDR US ARMY TACOM ARDEC
ATTN AMSRD AAR AEM A F BROWN
BLDG 151
PICATINNY ARSENAL NJ 07806-5000

1 CDR US ARMY TACOM ARDEC
ATTN AMSRD AAR AEM C A MOCK
BLDG 171A
PICATINNY ARSENAL NJ 07806-5000

1 CDR US ARMY TACOM ARDEC
ATTN AMSRD AAR AEM C J POTUCEK
BLDG 61S
PICATINNY ARSENAL NJ 07806-5000

1 CDR US ARMY TACOM ARDEC
ATTN AMSRD AAR AEP S PEARCY
BLDG 94
PICATINNY ARSENAL NJ 07806-5000

1 CDR US ARMY TACOM ARDEC
ATTN AMSRD AAR AEP M CILLI
BLDG 382
PICATINNY ARSENAL NJ 07806-5000

5 CDR US ARMY TACOM ARDEC
ATTN AMSRD AAR AEP E J VEGA
P GRANGER D CARLUCCI
M HOLLIS J KALINOWSKI
BLDG 94
PICATINNY ARSENAL NJ 07806-5000

NO. OF
COPIES ORGANIZATION

7 CDR US ARMY TACOM ARDEC
ATTN AMSRD AAR AEP E D TROAST
BLDG 171
PICATINNY ARSENAL NJ 07806-5000

2 CDR US ARMY TACOM ARDEC
ATTN AMSRD AAR AEP F H RAND
BLDG 61S
PICATINNY ARSENAL NJ 07806-5000

2 CDR US ARMY TACOM ARDEC
ATTN AMSRD AAR AEP F D PASCUA
BLDG 65S
PICATINNY ARSENAL NJ 07806-5000

2 CDR US ARMY TACOM ARDEC
ATTN AMSRD AAR AEP I
S LONGO C HALKIAS
BLDG 65S
PICATINNY ARSENAL NJ 07806-5000

4 CDR US ARMY TACOM ARDEC
ATTN AMSRD AAR AEP S N GRAY
M MARSH Q HUYNH
T ZAPATA
BLDG 94
PICATINNY ARSENAL NJ 07806-5000

1 CDR US ARMY TACOM ARDEC
ATTN AMSRD AAR AEP S C PEREIRA
BLDG 192
PICATINNY ARSENAL NJ 07806-5000

5 CDR US ARMY TACOM ARDEC
ATTN AMSRD AAR AEM L
M LUCIANO
G KOLASA M PALATHINGAL
D VO A MOLINA
BLDG 65S
PICATINNY ARSENAL NJ 07806-5000

1 CDR US ARMY TACOM ARDEC
ATTN AMSRD AAR AEM L R CARR
BLDG 1
PICATINNY ARSENAL NJ 07806-5000

1 CDR US ARMY TACOM ARDEC
ATTN AMSRD AAR AEM L J STRUCK
BLDG 472
PICATINNY ARSENAL NJ 07806-5000

NO. OF
COPIES ORGANIZATION

1 CDR US ARMY TACOM ARDEC
ATTN SFAE SDR SW IW B D AHMAD
BLDG 151
PICATINNY ARSENAL NJ 07806-5000

1 CDR US ARMY TACOM ARDEC
ATTN SFAE AMO CAS EX C GRASSANO
BLDG 171A
PICATINNY ARSENAL NJ 07806-5000

3 PRODUCT MANAGER FOR MORTARS
ATTN SFAE AMO CAS MS G BISHOP
P BURKE D SUPER
BLDG 162 SOUTH
PICATINNY ARSENAL NJ 07806-5000

1 PRODUCT MANAGER FOR MORTARS
ATTN SFAE AMO CAS MS J TERHUNE
BLDG 354
PICATINNY ARSENAL NJ 07806-5000

3 CDR US ARMY TACOM ARDEC
ATTN SFAE AMO CAS R KIEBLER
M MORATZ A HERRERA
BLDG 171A
PICATINNY ARSENAL NJ 07806-5000

3 CDR NAVAL SURF WARFARE CTR
ATTN G34 M TILL G34 H WENDT
G34 M HAMILTON
G34 S CHAPPELL
17320 DAHLGREN ROAD
DAHLGREN VA 22448-5100

3 CDR NAVAL SURF WARFARE CTR
ATTN G34 J LEONARD
G34 W WORRELL
G34 M ENGEL
17320 DAHLGREN ROAD
DAHLGREN VA 22448-5100

4 CDR NAVAL SURF WARFARE CTR
ATTN G61 E LARACH G61 M KELLY
G61 A EVANS
17320 DAHLGREN ROAD
DAHLGREN VA 22448-5100

1 CDR OFC OF NAVAL RSCH
ATTN CODE 333 P MORRISON
800 N QUINCY ST RM 507
ARLINGTON VA 22217-5660

NO. OF
COPIES ORGANIZATION

1 DIR NAVAL AIR SYSTEMS CMD
TEST ARTICLE PREP DEP
ATTN CODE 5 4 R FAULSTICH
BLDG 1492 UNIT 1
47758 RANCH RD
PATUXENT RIVER MD 20670-1456

1 CDR NAWC WEAPONS DIV
ATTN CODE 543200E G BORGEN
BLDG 311
POINT MUGU CA 93042-5000

2 PROGRAM MANAGER ITTS
PEO-STRI
ATTN AMSTI EL D SCHNEIDER
C GOODWIN
12350 RESEARCH PKWY
ORLANDO FL 32826-3276

2 CDR US ARMY RDEC
ATTN AMSRD AMR SG SD P JENKINS
AMSRD AMR SG SP P RUFFIN
BLDG 5400
REDSTONE ARSENAL AL 35898-5247

1 DIR US ARMY RTTC
ATTN STERT TE F TD R EPPS
REDSTONE ARSENAL AL 35898-8052

1 ARROW TECH ASSOCIATES
ATTN W HATHAWAY
1233 SHELBURNE RD STE 8
SOUTH BURLINGTON VT 05403

5 ALLIANT TECHSYSTEMS
ATTN A GAUZENS J MILLS
B LINDBLOOM E KOSCO
D JACKSON
PO BOX 4648
CLEARWATER FL 33758-4648

1 ALLIANT TECHSYSTEMS
ATTN R DOHRN
5050 LINCOLN DR
MINNEAPOLIS MN 55436-1097

5 ALLIANT TECHSYSTEMS
ATTN G PICKUS F HARRISON
M WILSON (3 CYS)
4700 NATHAN LANE NORTH
PLYMOUTH MN 55442

NO. OF
COPIES ORGANIZATION

8 ALLIANT TECHSYSTEMS
ALLEGANY BALLISTICS LAB
ATTN S OWENS C FRITZ J CONDON
B NYGA
J PARRILL M WHITE
S MCCLINTOCK K NYGA
MAIL STOP WV01-08 BLDG 300
RM 180
210 STATE ROUTE 956
ROCKET CENTER WV 26726-3548

2 SAIC
ATTN J DISHON
16701 W BERNARDO DR
SAN DIEGO CA 92127

3 SAIC
ATTN J GLISH J NORTHRUP
G WILLENBRING
8500 NORMANDEALE LAKE BLVD
SUITE 1610
BLOOMINGTON MN 55437-3828

1 SAIC
ATTN D HALL
1150 FIRST AVE SUITE 400
KING OF PRUSSIA PA 19406

1 AAI CORPORATION
M/S 113/141
ATTN C BEVARD
124 INDUSTRY LANE
HUNT VALLEY MD 21030

2 JOHNS HOPKINS UNIV
APPLIED PHYSICS LABORATORY
ATTN W D'AMICO K FOWLER
1110 JOHNS HOPKINS RD
LAUREL MD 20723-6099

4 CHLS STARK DRAPER LAB
ATTN J CONNELLY J SITOMER
T EASTERLY A KOUREPENIS
555 TECHNOLOGY SQUARE
CAMBRIDGE MA 02139-3563

2 ECIII LLC
ATTN R GIVEN J SWAIN
BLDG 2023E
YPG AZ 85365

NO. OF
COPIES ORGANIZATION

1 GD-OTS
ATTN E KASSHEIMER
PO BOX 127
RED LION PA 17356

1 ALION SCIENCE
ATTN P KISATSKY
12 PEACE RD
RANDOLPH NJ 07861

ABERDEEN PROVING GROUND

1 DIRECTOR US ARMY RSCH
LABORATORY
ATTN AMSRD ARL CI OK (TECH LIB)
BLDG 4600

1 DIRECTOR US ARMY RSCH
LABORATORY
ATTN AMSRD ARL SG
T ROSENBERGER
BLDG 4600

17 DIR USARL
ATTN AMSRD ARL WM BA D LYON
T BROWN E BUKOWSKI
J CONDON B DAVIS
R HALL T HARKINS (5 CYS)
D HEPNER G KATULKA
T KOGLER P MULLER
B PATTON P PEREGINO
BLDG 4600

3 DIR USARL
ATTN AMSRD ARL WM BC
P PLOSTINS
B GUIDOS P WEINACHT
BLDG 390

3 DIR USARL
ATTN AMSRD ARL WM BD M NUSCA
J COLBURN T COFFEE
BLDG 390

2 DIR USARL
ATTN AMSRD ARL WM BF
W OBERLE A THOMPSON
BLDG 390

2 DIR USARL
ATTN AMSRD ARL WM MB
J BENDER W DRYSDALE
BLDG 390

NO. OF
COPIES ORGANIZATION

2 DIR USARL
ATTN AMSRD ARL WM T B BURNS
ATTN AMSRD ARL WM TC R COATES
BLDG 309

4 CDR US ARMY TACOM ARDEC
ATTN AMSRD AAR AEF T
R LIESKE J MATTS
F MIRABELLE J WHITESIDE
BLDG 120

2 CDR ABERDEEN TEST CENTER
ATTN CSTE DTC AT TD B
K MCMULLEN
CSTE DTC AT SL B D DAWSON
BLDG 359

2 CDR ABERDEEN TEST CENTER
ATTN CSTE DTC AT FC L R SCHNELL
J DAMIANO
BLDG 400

1 CDR ABERDEEN TEST CENTER
ATTN CSTE DTC AT TD S WALTON
BLDG 359

1 CDR USAEC
ATTN CSTE AEC SVE B D SCOTT
BLDG 4120